Optimization of Aircraft Structures and Rotating Machinery

Professor J. S. Rao
Director Advanced Engineering
Altair Engineering India
Bangalore
js.rao@altair.com

ABSTRACT

Recent advances in optimization processes have enabled rapid and accurate weight reduction of stationary aircraft structures and shape optimization of rotating bladed disk grooves to minimize the local strains for increased life. India's capabilities in this sector will be described.

INTRODUCTION

Weight reduction in stationary structural components, wings and fuselage of an aircraft is always the goal of the modern day designers. Altair developed in recent years a linear structural code for optimization *Altair OptiStruct* together with *Altair HyperMesh* which has been successfully employed in reducing the weight of Airbus 380 wings by as much as 500 kg amongst others. In this paper, we will present the methodology of weight reduction through an example of a wing box rib of an airframe keeping the structural integrity of a given base line.

Aircraft engines are designed to operate in limit subjecting the rotors to near plastic conditions at the discontinuities or notch locations. These structures are globally elastic and locally plastic and the local strains play a major role in limiting the mission life. *Altair HyperStudy* is a multi-physics platform for optimization of solids and fluids including nonlinearities. A typical rotating bladed disk under local plastic conditions is considered with a base line designed from testing and experience. The groove shape is optimized to provide considerable reduction in plastic strain by as much as 26%. The procedure for such an optimization is presented.

OPTIMIZATION

Optimization problems are classified as given in Table 1, see Rao [1]. An optimization problem in general requires, defining an objective function, design constraints and design variables. The optimization may be based on multi objective functions. The physical problem may be governed by Linear equations, i.e., Linear Programming, Quadratic Programming, Geometric Programming or Nonlinear Programming. It could also be stochastic in nature.

Table 1 Classification of Optimization Problems

Constraints	Design Variables	Physical Structure	Nature of Equations
Constrained Equality and Inequality	Parameter or Static	Optimal Control	Nonlinear Programming
Unconstrained	Dynamic – Design Variables continuous function through space	Non Optimal	Geometric Programming
			Quadratic Programming
			Linear Programming
Multi-objective Programming		Stochastic Programming	

To understand the basic principles, a simple example is first illustrated. Design a column such that Stress induced is < yield and buckling; Mean diameter d to be in the range 2 to 14 cm; Thickness t to be in the range 0.2 to 0.8 cm; Cost to be lowest, given by 5 times weight + 2 times the mean diameter. Material properties are E = 0.85E+06 kg/cm2, Density = 0.0025 kg/cm2 and Yield stress = 500 kg/cm^2, Length l = 250 cm with the load P = 2500 kg. Mathematically the optimization problem is

Design Vector $X = \begin{Bmatrix} x_1 \\ x_2 \end{Bmatrix} = \begin{Bmatrix} d \\ t \end{Bmatrix}$

Objective Function $f(X) = 5W + 2d = 5\rho l \pi dt + 2d = 9.82 x_1 x_2 + 2x_1$

Behavioral Constraints:

induced stress ≤ yield stress

$$\frac{P}{\pi dt} = \frac{2500}{\pi x_1 x_2} \le 500$$

$$g_1(X) = \frac{2500}{\pi x_1 x_2} - 500 \le 0$$

$$\Rightarrow x_1 x_2 \ge 1.593 \qquad \text{Plot } P_1\ Q_1 \quad x_1 x_2 = 1.593$$

induced stress ≤ buckling stress

$$\frac{2500}{\pi x_1 x_2} \le \frac{\pi^2 \left(0.85 \times 10^6\right)\left(x_1^2 + x_2^2\right)}{8(250)^2}$$

$$g_2(X) = \frac{2500}{\pi x_1 x_2} - \frac{\pi^2 \left(0.85 \times 10^6\right)\left(x_1^2 + x_2^2\right)}{8(250)^2} \le 0$$

$$\Rightarrow x_1 x_2 \left(x_1^2 + x_2^2\right) = 47.3 \quad \text{Plot } P_2\ Q_2$$

Side Constraints:

$2.0 \le d \le 14.0$

$0.2 \le t \le 0.8$

$$g_3(X) = -x_1 + 2.0 \le 0$$
$$g_4(X) = x_1 - 14.0 \le 0$$
$$g_5(X) = -x_2 + 0.2 \le 0$$
$$g_6(X) = x_2 - 0.8 \le 0$$

The graphical solution of the above single objective function with two design variables, two behavioral constraints and four side constraints is illustrated in Fig. 1 which is self explanatory.

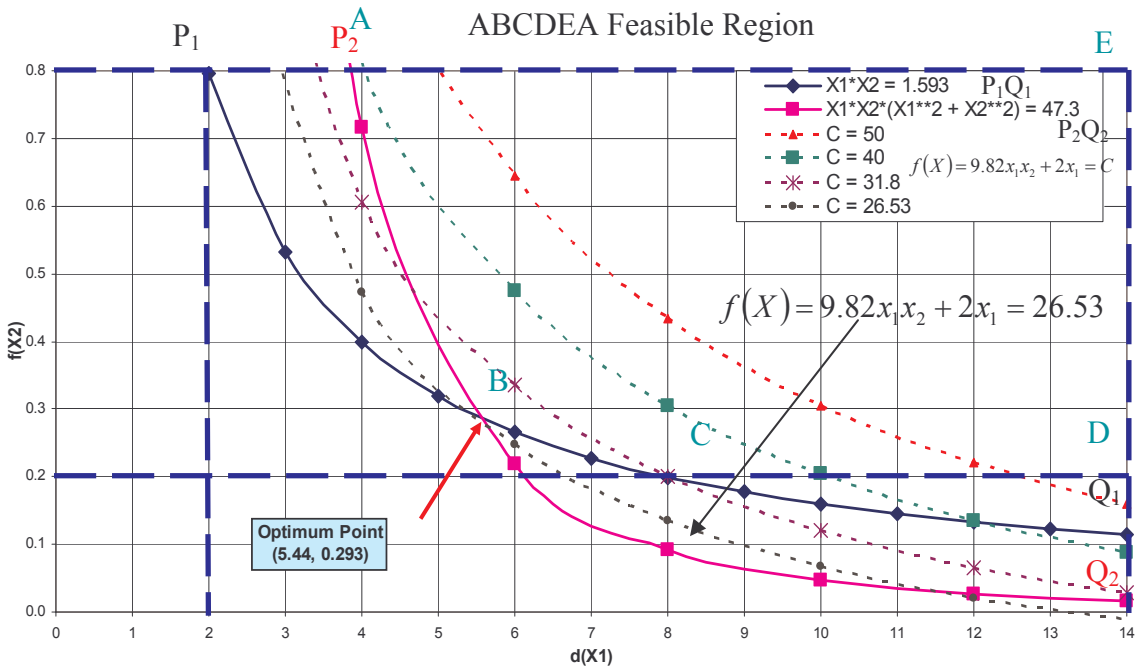

Fig. 1 Single Objective Function Graphical Solution with Two Design Variables and Two Behavioral Constraints and Four Side Constraints

Altair OptiStruct is specially designed as a linear finite element solver; see [2] that uses an iterative procedure known as the local approximation method to solve the optimization problem. The design update is computed using the solution of an approximate optimization problem, which is established using the sensitivity information. *Altair OptiStruct* has three different methods implemented: the optimality criteria method, a dual method, and a primal feasible directions method. The primal method is more common in shape optimizations. This approach is based on the assumption that only small changes occur in the design with each optimization step.

Altair developed a multipurpose DOE/Optimization/Stochastic tool *HyperStudy* [3] that can be applied in the multi-disciplinary optimization of a design combining different analysis types. Once the finite element model and shape variables are developed, an optimization can be performed by linking *Altair HyperStudy* to a particular solver of choice that can include nonlinear analyses. It uses global optimization methods which is very general in that they can be used with any analysis code, including non-linear analysis codes. Global optimization methods use higher order polynomials to approximate the original structural optimization problem over a wide range of design variables. The polynomial approximation techniques are referred to as Response Surface methods. A sequential response surface method approach is used in which, the objective and constraint functions are approximated in terms of design variables using a second order polynomial. One can create a sequential response surface update by linear steps or by quadratic response surfaces. The process can also be used for non-linear physics and experimental analysis using wrap-around software, which can link with various solvers.

The solution of the optimization problem obtained by *Altair HyperStudy* is shown in Figs. 2a and 2b.

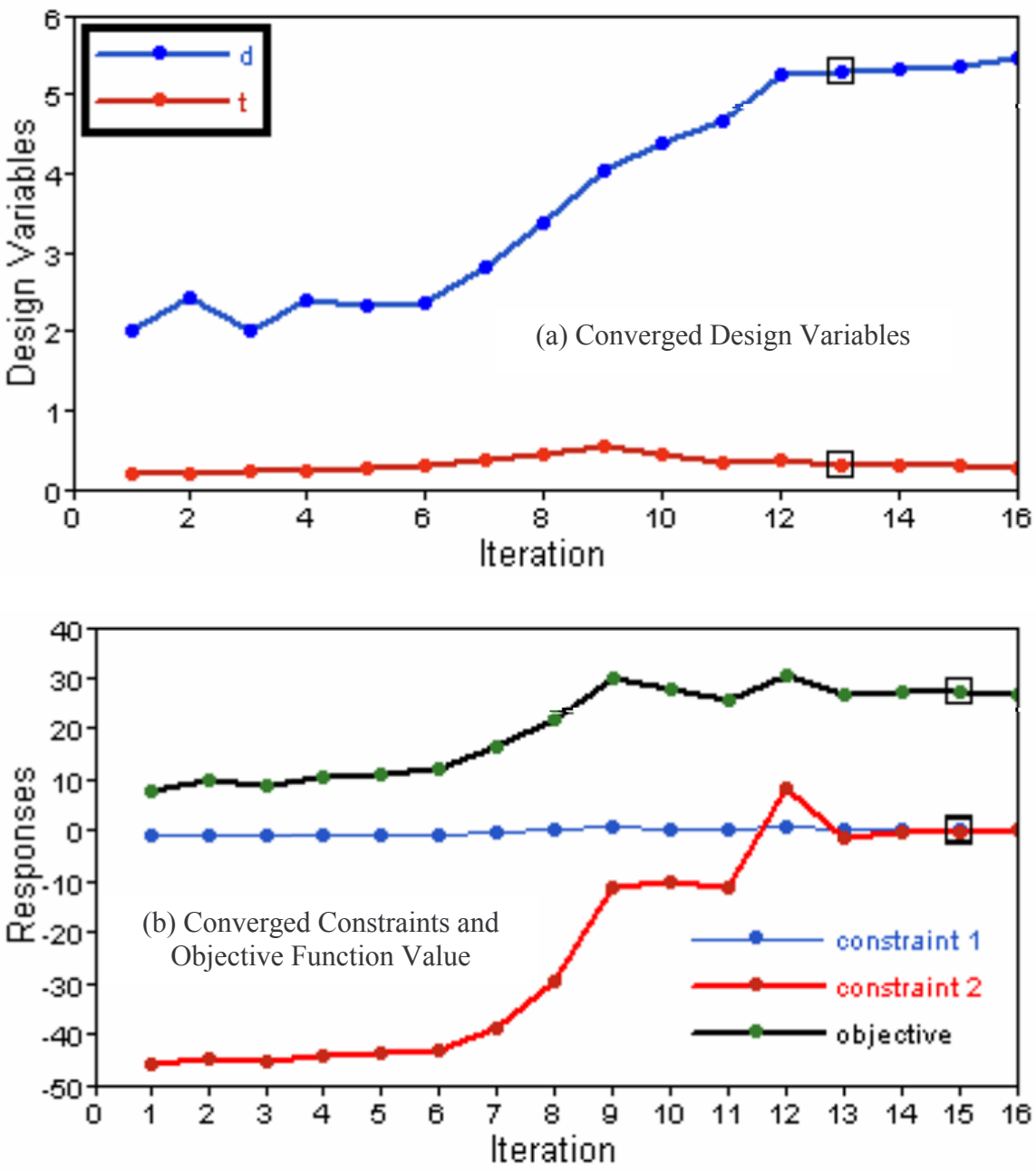

Fig. 2 *HyperStudy* Optimization in 16 Iterations of the Graphical Solution in Fig. 1

AIRCRAFT STRUCTURES TOPOLOGY OPTIMIZATION

The optimization process of a typical aircraft nose rib is illustrated in Fig. 3. Typically it starts with the base line of an operating structure in service or a component being newly designed. The base line model is defined with the design space and external

loads. The design space is filled with small virtual cubes with the help of *Altair HyperMesh* [4]. *Altair OptiStruct* is a linear structural code that is next used to identify the load flow path and vacant space (topology optimization) where the material is unnecessary from a functional point of view.

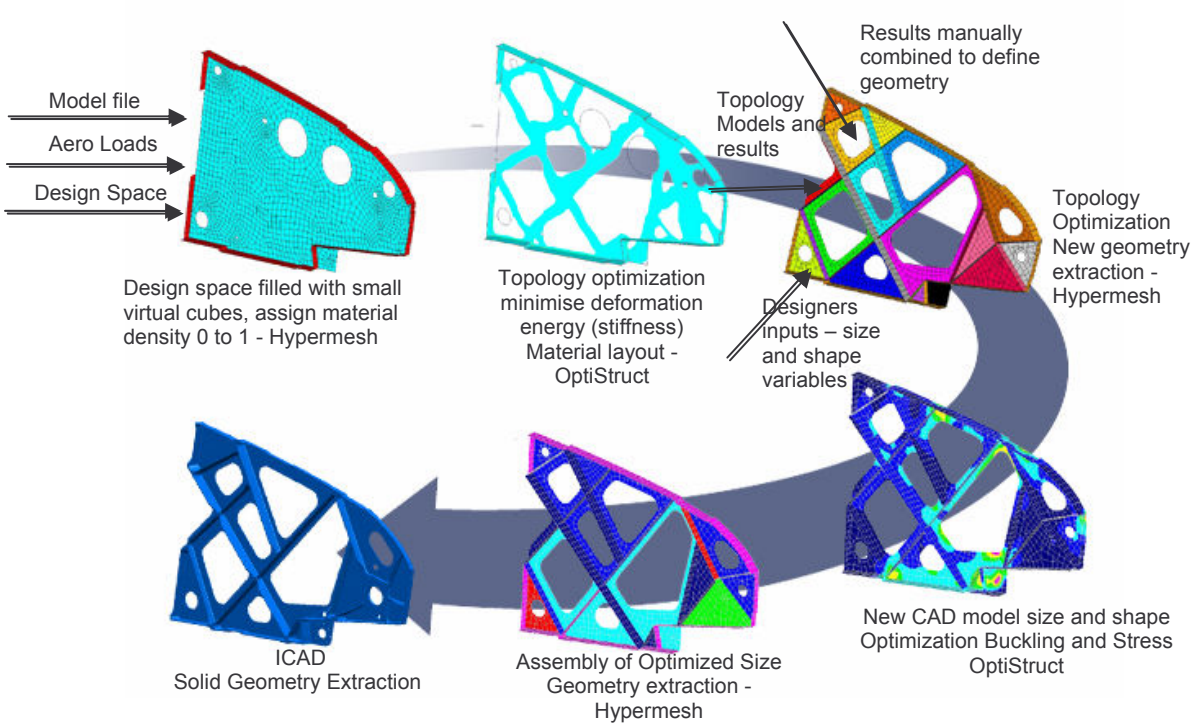

Fig. 3 Topology Optimization Process Illustrated for a Nose Rib

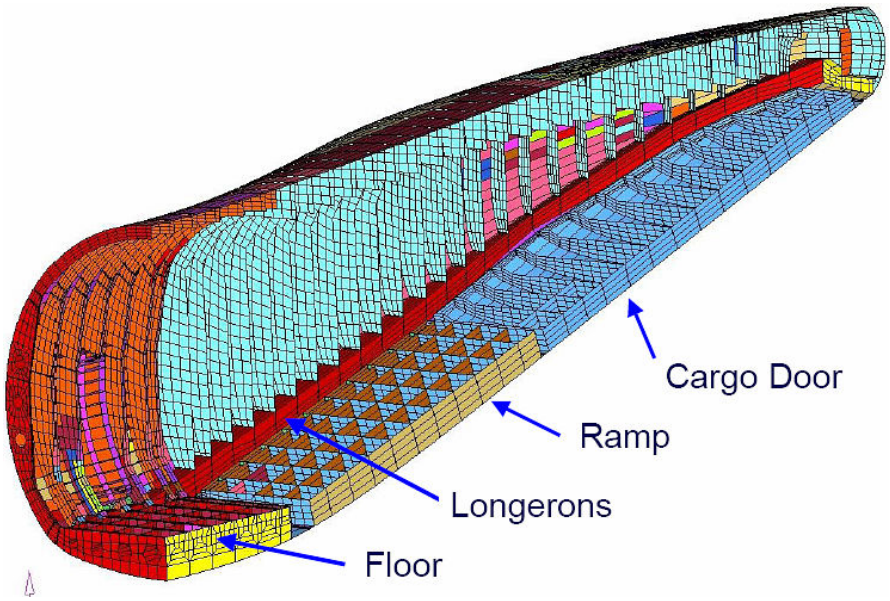

Fig. 4 A400 M Military Transport Aircraft FE Model for Optimization

This technology has helped in considerable weight reduction by 500 kg in Airbus 380 wings [5], A400 M Military Transport aircraft shown in Fig. 4 [6] and similar reductions in F-35 Joint Strike Fighter [7].

A typical rib of an aircraft wing box is shown in Fig. 5. The FE model of this base line rib is then subjected to aerodynamic drag and Jack loads during landing as shown in Fig. 6 to determine the peak stress and displacement which are 97.7 MPa and 1.062 mm respectively. The first topology optimization resulted in the flow path as shown by relative density plot in Fig. 7. Inputs from engineering team are taken to select areas in material density region 0 to 0.3 and make additional cutouts and thinning the ribs and topology iterations carried out to give the final optimized rib shown in Fig. 8. This rib has same displacement and stress peak values as the base line however the weight is reduced from 8.085 kg to 3.75 kg thus giving a weight saving by ~ 46% [8].

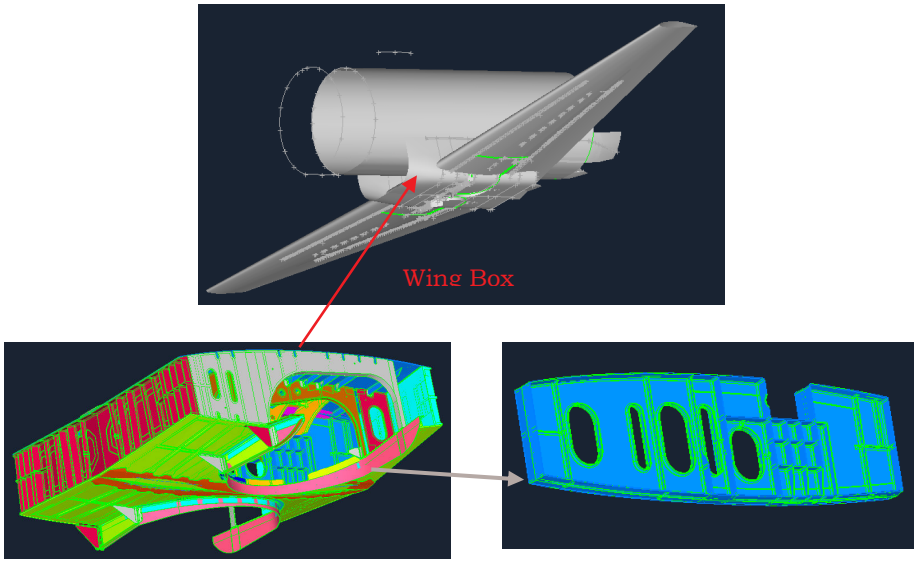

Fig. 5 Base Line Wing Box Rib for Optimization

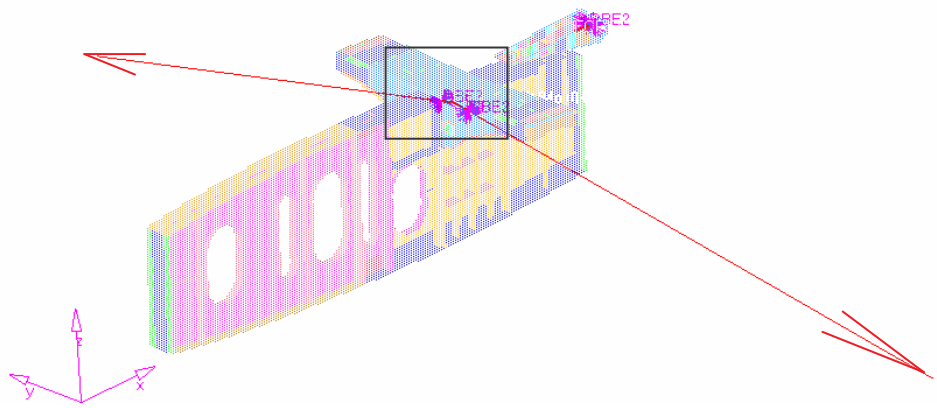

Fig. 6 FE Model of Rib and Loads

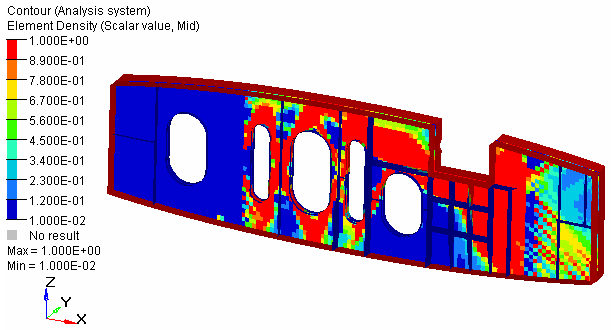

Fig. 7 Topology Optimization and Relative Material Density

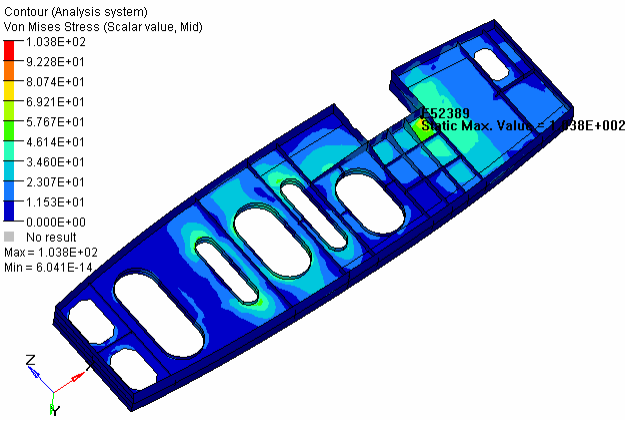

Fig. 8 Optimized Rib

ROTATING MACHINERY SHAPE OPTIMIZATION

An axial entry LP turbine blade having a fir tree root design is chosen. A sector of rotor disc is modeled to make use of cyclic symmetry condition. The Blade is pre-twisted with a height of 290 mm. There are 60 blades in this LP stage and are placed on the disk with the bottom of the blade root at a radius of 248 mm from the axis of the rotor. A 3-D finite element model of the bladed disc is generated as shown in Fig. 9. Using mapped meshing options a solid element mesh with 8 nodes is generated, by capturing all the critical regions with finer mesh. Mesh around the singularities, blade and disc dovetail root fillet regions at higher radius, where the peak stresses are expected are captured with 2 to 3 layers of elements with element size as low as 0.235 mm. The mesh shown consists of 305524 elements and 344129 nodes.

Baseline Analysis

For the analysis the blade along with disk effect is considered by modeling a 1/60 sector of the disk with one blade and using cyclic symmetry boundary conditions applied on both the partition surfaces as shown in Fig. 9. The common nodes on the pressure faces at six positions, shown in Fig. 9, where the load transfer between blade and disc takes place are joined together to make it as a single entity. The blade and disc are

assumed to be made up of same material with Yield stress of 585 MPa, Young's Modulus 210 GPa, Density 7900 Kg/m^3 and Poisson's Ratio 0.3.

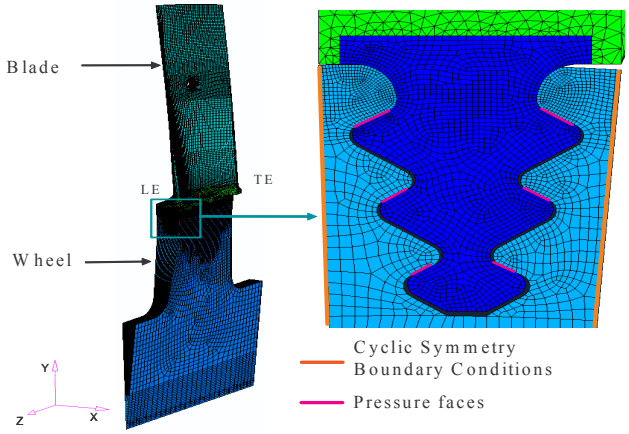

Fig.9 Bladed Disk Model Showing the FE Mesh

An elastic stress analysis is conducted for a centrifugal load at full speed 8500 RPM, using ANSYS solver [9]. The Von Mises elastic stress field near the root region is shown in Fig. 10. The root fillet in the first landing area experiences a severe stress of 1825 MPa at node 153608 well beyond Yield 585 MPa, with an average sectional stress 256 MPa. Stress contour beyond yield is shown to be spread across 3 elements over a depth of 1.22 mm.

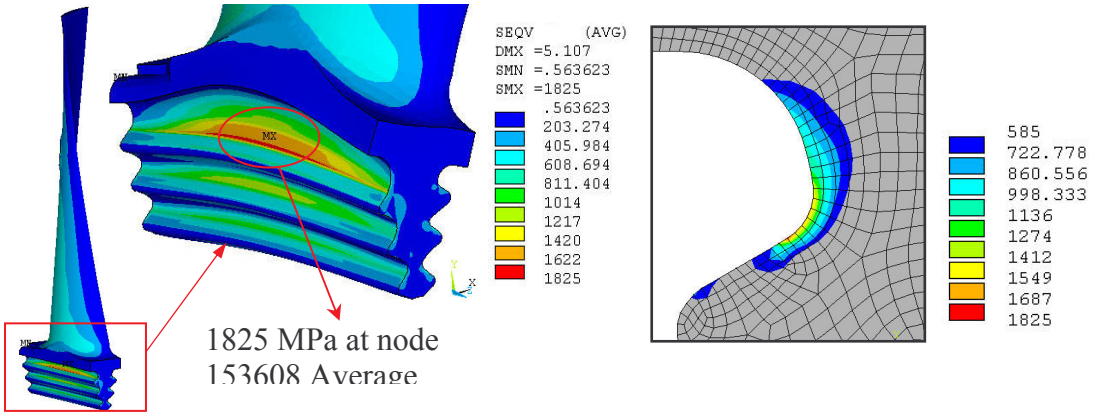

Fig.10 Von Mises Stress in Elastic domain at 8500 RPM

The hardening property of the material in the plastic region is given in Fig. 11. To have a better understanding on the plastic region, next an elasto-plastic stress analysis is carried out. The elasto-plastic analysis result for the von Mises stress is given in Fig. 12. The stress region beyond yield is also defined in the same figure. The root fillet now experiences a peak Von Mises stress 768 MPa at a node 176017 in the same region which is beyond the yield value 585 MPa. From Fig. 12, it is observed that the plastic region has not changed from the simple elastic analysis result in Fig. 10. The peak stress value has dropped considerably from the elastic analysis result 1825 MPa to a value 768 MPa just above the yield.

The material in the root region around the stress raiser location flows thus easing the stress and raising the strain in accordance to the hardening law given in Fig. 11. The peak strain observed at the node 153608 in the same region closer to peak stress location is 0.0153.

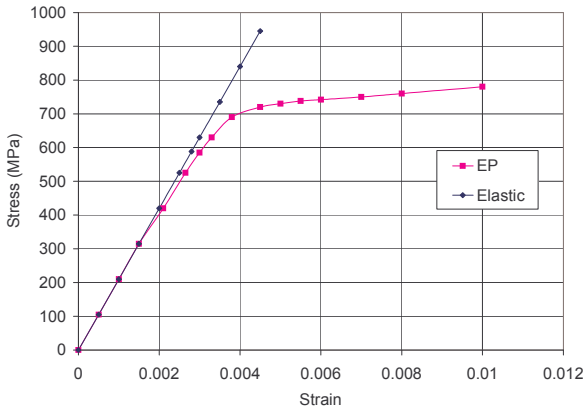

Fig.11 Material hardening characteristic in the plastic region

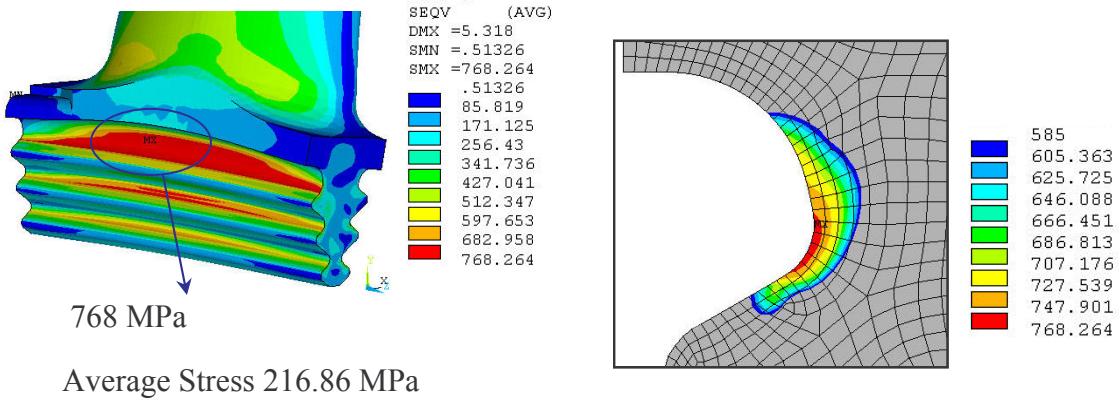

Average Stress 216.86 MPa

Fig.12 Results of Elasto-Plastic analysis at 8500 RPM

Altair OptiStruct is a linear stress analysis code and optimization is possible when the structure is wholly elastic as against the globally elastic and locally plastic condition in Fig. 12. The location where peak stress occurs remains almost the same depending on the stress raiser location irrespective of the loading condition. Therefore, the shape optimization can be as well conducted at a speed where the structure is wholly elastic and verify the conditions at full speed under elasto plastic conditions. This will also reduce the computational time. Therefore an elastic stress analysis is carried out for centrifugal load at 4000 RPM. Fig. 13 shows the Von Mises stress distribution obtained which is completely elastic. The peak stress observed is 404 MPa in the root fillet of the blade at the same node number as observed before

Optimization through *OptiStruct*

Shape variables are generated using mesh morphing technique in *Altair HyperMesh*. Using the baseline finite element model in Fig. 9, a suitable number of

shapes in the vicinity of baseline consistent with the available design space is defined by modifying the grid point locations, which are saved as perturbation vectors. The shapes generated are combinations of parameters shown in Fig. 14. Shapes are then defined as variables by assigning the lower and upper bounds to it. Table 2 gives the minimum and maximum values adopted for defining the shape variables. Shape variables can then be assigned as indicated to perturbation vectors, which control the shape of the model within a given bound. This is helpful in generating the required shape bounds without re-meshing the model.

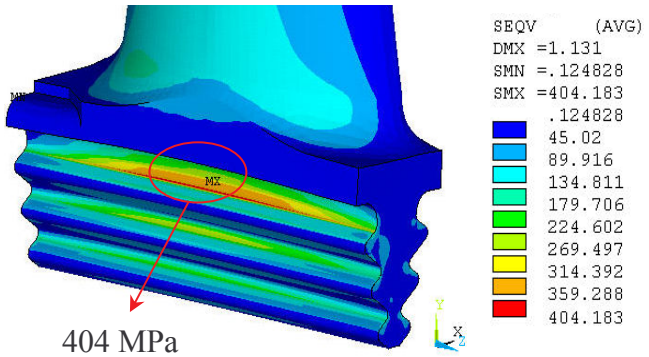

Fig.13 Von Mises Stress in Elastic domain at 4000 RPM

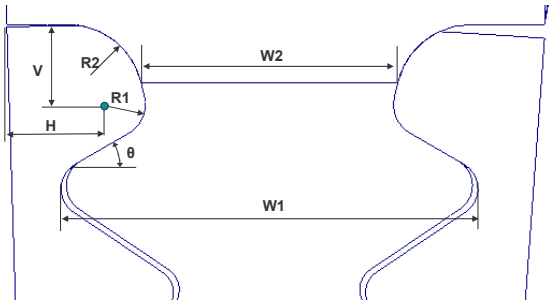

Fig. 14 Parameters used for defining the shape variables

Shape Optimization is then carried out using *Altair OptiStruct* code at two speeds, 4000 and 8500 RPM, see [10]. The cyclic symmetry boundary conditions are simulated by using enforced displacements obtained from baseline analysis. The optimized result for 4000 RPM is shown in Fig. 15. The peak stress obtained is 323 MPa as against the base line value 404 MPa given in Fig. 13 giving a drop of 20% in the optimized shape.

Table.2 Shape Variable Definitions

Minimum Value (mm)	Maximum Value (mm)
W1 = 22.17	W1 = 25.76
W2 = 13.65	W2 = 13.86
R1 = 1.70, H = 5.67, V = 4.13, R2 = 4.0	R1 = 2.14, H = 4.85, V = 4.06, R2 = 3.37
$\theta = 29.86^0$	$\theta = 16.25^0$

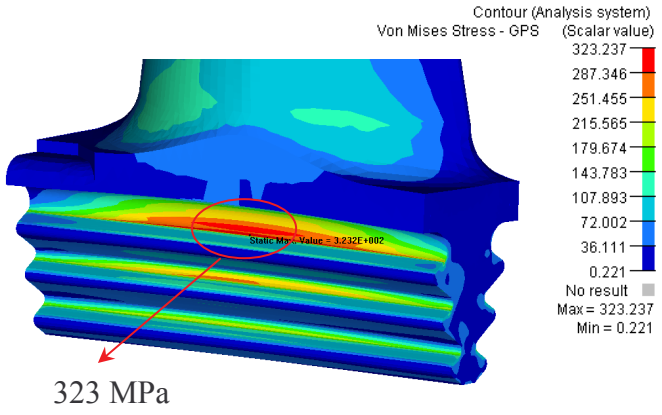

Fig. 15 Von Mises Stress at 4000 RPM for Optimized configuration

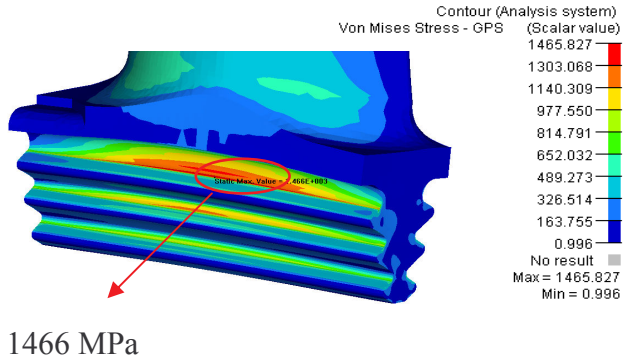

Fig. 16 Von Mises Stress at 8500RPM for Optimized configuration

Table 3 Optimized Shapes at 4000 and 8500 RPM

Baseline Configuration (mm)	Optimized Shape (mm) 4000RPM	Optimized Shape (mm) 8500RPM
W1 = 22.17	W1 = 25.72	W1 = 25.72
W2=13.65	W2 = 13.86	W2 = 13.86
R1 = 1.70, H = 5.67, V = 4.13, R2 = 4.0	R1 =1.95, H = 5.05, V = 4.03, R2 = 3.97	R1 = 2.10, H = 4.91, V = 4.04, R2 = 3.98
$\theta = 29.86^0$	$\theta = 16.25^0$	$\theta = 16.25^0$

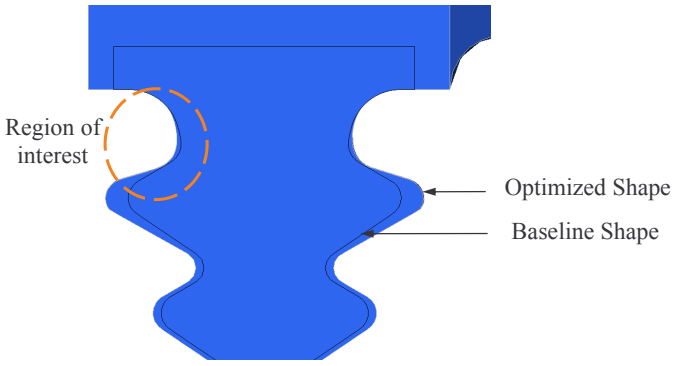

Fig. 17 Blade Root profiles of Baseline and Optimized configuration

The optimized result for 8500 RPM is shown in Fig. 16. The peak stress obtained is 1466 MPa as against the base line value 1825 MPa given in Fig. 10 giving a drop of 19.5% similar to 4000 RPM run in the optimized shape. In both the cases, the optimized shape obtained is same as given in Fig. 17 where the result is compared with the baseline and in Table 3 where the shape variable values achieved for both the speeds are presented. The stress concentration factor obtained in either of the speeds is around 7.12 as can be seen from Figs. 10 and 13. When linear elasticity is adopted for calculations, the peak stress is magnified by the stress concentration factor irrespective of the local condition elastic or plastic. Under plastic conditions, we have to account for material flow that relaxes the stress and raises the strain.

Optimization through HyperStudy

Here shape optimization by using elastic and elasto-plastic material properties is discussed. Shape optimization is carried by using the baseline model, having the cyclic symmetry boundary conditions imposed on the disc, with the objective to minimize the peak stresses. Shape variables generated previously are used as design variables. Optimization is carried out at two speeds, 4000 and 8500 RPM, with elastic properties.

Von Mises elastic stress field of the optimized shapes is shown Fig. 18. Maximum stress has decreased from 404 to 325 MPa by 79 MPa (19.5% as against 20% achieved in *OptiStruct*) from baseline for 4000 RPM and from 1825 to 1501 MPa by 325 MPa (17.7% as against 19.5% achieved in *OptiStruct*) for 8500 RPM from complete elastic analysis. Note that the analysis in this study is more accurate as the cyclic symmetry conditions are directly applied instead of cut boundary conditions in *OptiStruct* analysis. The blade root profile obtained from the optimization is shown in Fig. 19.

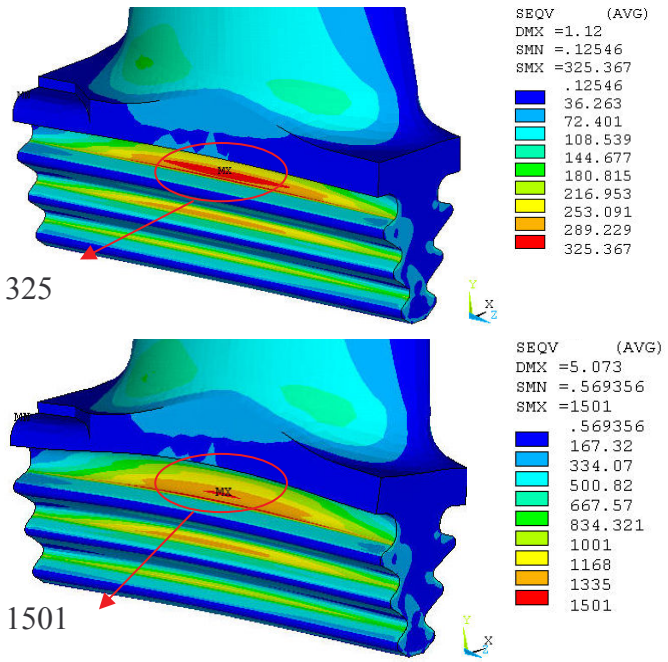

Fig. 18 Von Mises Stress at 4000 & 8500RPM for Optimized Configuration

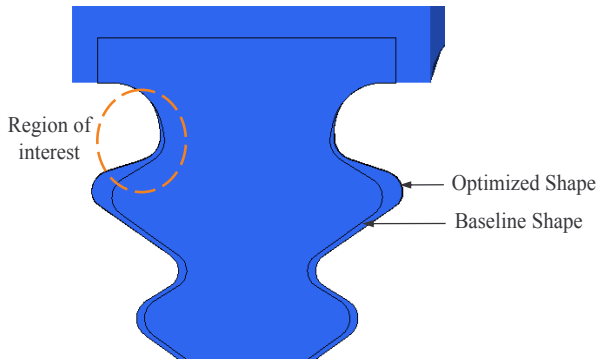

Fig. 19 Blade Root profiles of Baseline and Optimized Configuration

The variation of peak stress and shape variables in iteration is shown in Fig.20.

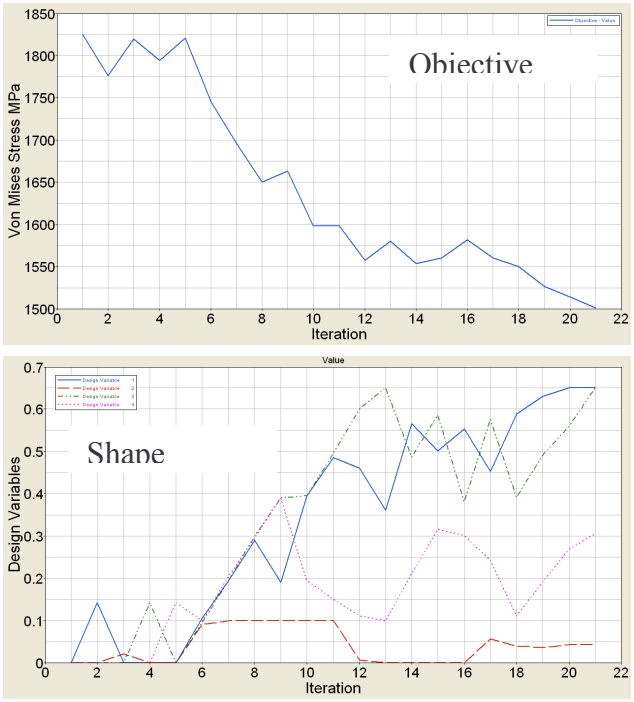

Fig. 20 Variation of Objective and Shape variables during optimization

Next, a shape optimization was carried out using elasto-plastic material properties at 8500 RPM to asses the actual optimization result under plastic conditions. The Von Mises stress distribution for the optimized shape is shown in Fig. 21. Maximum stress has decreased marginally from 768 to 746 MPa by 22 MPa (2.86%) from baseline elasto-plastic analysis for 8500 RPM; however the peak plastic strains reduced from 0.0153 to 0.01126 by 26.4%. This is the major advantage in optimization for a blade root shape.

Many existing machines have roots designed by experience and there can be considerable margin in lowering peak strains and therefore enhanced life. Table 4 shows the optimized shapes obtained from elastic and elasto-plastic analyses which are in close match.

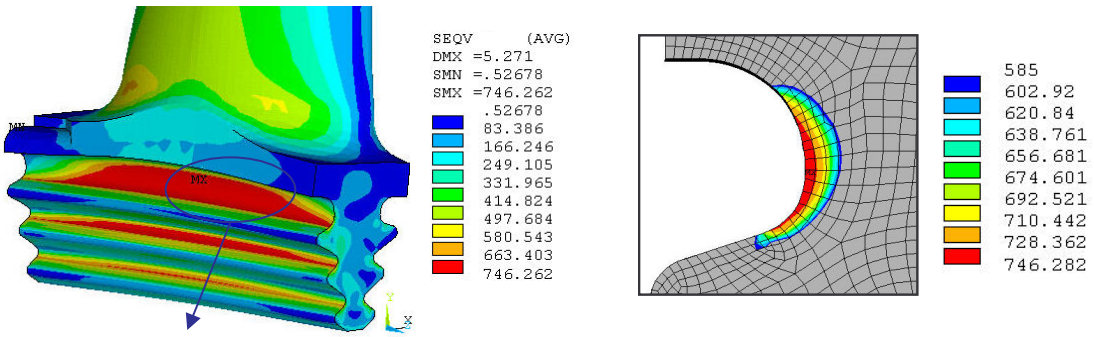

Von Mises Stress 746 MPa

Fig. 21 Results of Elasto-Plastic analysis at 8500 RPM for Optimized Configuration

Table 4 Comparison of Baseline and Optimized Configuration

Baseline Configuration (mm)	Optimized Shape (mm) 4000RPM
W1 = 22.17	W1 = 25.36
W2 = 13.65	W2 = 13.86
R1 = 1.70, H = 5.67, V = 4.13, R2 = 4.0	R1 = 1.74, H = 5.29, V = 3.90, R2 = 4.0
$\theta = 29.86^0$	$\theta = 16.25^0$

Optimized Shape (mm) 8500RPM	Optimized Shape (mm) 8500RPM - EP
W1 = 25.43	W1 = 25.48
W2 = 13.86	W2 = 13.82
R1 = 1.89, H = 5.17, V = 4.01, R2 = 4.0	R1 = 2.08, H = 4.96, V = 4.07, R2 = 4.0
$\theta = 16.50^0$	$\theta = 17.15^0$

CONCLUDING REMARKS

Optimization has become inevitable in aircraft structures and rotating machinery to reduce weight and push the designs into limiting values. The earlier practice has been prototype building and testing until the desired safe systems are achieved. This is not only very time consuming but also expensive. Advanced analysis has helped in accurate simulation but the design cycle time remained high because optimization procedures have not been available to handle multi physics objectives with thousands of design variables of nonlinear systems. This design cycle time has been now kept to a minimum through advanced optimization codes to achieve light weight stationary and rotating structures with enhanced life.

ACKNOWLEDGMENTS

The author is thankful to Altair Engineering India and several young colleagues for their support.

REFERENCES

1. Rao, Singiresu. S., *Engineering Optimization Theory and Practice*, 3rd Edition. John Wiley, 1996
2. *Altair OptiStruct, User's Manual v7.0*, Altair Engineering Inc., Troy, MI, 2003
3. *Altair HyperStudy, User's Manual v7.0*, Altair Engineering Inc., Troy, MI, 2003
4. *Altair HyperMesh, User's Manual v7.0*, Altair Engineering Inc., Troy, MI, 2003
5. Krog, L., Tucker, A. and Rollema, G., *Application of Topology, Sizing and Shape Optimization Methods to Optimal Design of Aircraft Components*, Altair Engineering Ltd., 2002
6. Stettner, M. and Schuhmacher, G. Optimization Assisted Design of Military Transport Aircraft Structures, *Altair Optimization Technology Conference, OTC04*, Troy, Michigan, September 23, 2004
7. Taylor, R. M., et. al., Detail Part Optimization on the F-35 Joint Strike Fighter, AIAA 2006-1868, *47th AIAA/ASME/ASCE/AHS/ASC Structures, Structural Dynamics, and Material Conference*, Newport, Rhode Island, 2006
8. Rao, J. S., Shape Optimization to improve Life of Bladed Disks in Turbomachinery, Invited address, International Conference on Trends in Product Lifecycle, Modelling, Simulation and Synthesis (PLMSS'06), December 16-18, 2006, Bangalore
9. ANSYS Release 9.0 Documentation, Ansys Inc., 2004
10. Rao, J. S. and Suresh, S., 2006, Blade Root Shape Optimization, The Future of Gas Turbine Technology, 3rd International Conference 11-12 October , S2-T2-3, Brussels, Belgium